ORIGINAL RESEARCH

Maturation of Thalamic Radiations between 34 and 41 Weeks' Gestation: A Combined Voxel-Based Study and Probabilistic Tractography with Diffusion Tensor Imaging

A. Aeby
Y. Liu
X. De Tiège
V. Denolin
P. David
D. Balériaux
M. Kavec
T. Metens
P. Van Bogaert

BACKGROUND AND PURPOSE: This study aimed to investigate brain maturation along gestational age with diffusion tensor imaging in healthy preterm and term neonates. Therefore, a voxel-based study of fractional anisotropy (FA) and mean diffusivity (D_{av}) was performed to reveal the brain regions experiencing microstructural changes with age. With tractography, the authors intended to identify which fiber tracts were included in these significant voxels.

MATERIALS AND METHODS: There were 22 healthy preterm and 6 healthy term infants who underwent MR imaging between 34 and 41 weeks of gestation. A statistical parametric approach was used to evidence the effect of age on regional distribution of FA and D_{av} values. The fiber tracts suspected to be included in the significant clusters of voxels were identified with neuroanatomy and tractography atlases, reconstructed with probabilistic tractography, and superimposed on the parametric maps.

RESULTS: Parametric analysis showed that FA increases with age in the subcortical projections from the frontal (motor and premotor areas) and parietal cortices, the centrum semiovale, the anterior and posterior arms of the internal capsules, the optic radiations, the corpus callosum, and the thalami ($P <$ .05, corrected). Superimposition of the parametric maps on tractography showed that the corticospinal tract (CST); the callosal radiations (CR); and the superior, anterior, and posterior thalamic radiations were included in the significant voxels. No statistically significant results were found for D_{av} maps.

CONCLUSIONS: These results highlight that, besides the already-evidenced FA increase in the CST and CR, the thalami and the thalamic radiations experience microstructural changes in the early development of the human brain.

Although cerebral development is an ongoing process from the early embryonic period to the second decade of postnatal life, rapid and important developmental changes occur between the third trimester of gestation and the first postnatal months.[1] Structural changes underlying this process can be evidenced with conventional MR imaging,[2] but this technique is not sensitive enough to evaluate microstructural changes associated with white matter organization and maturation.

Diffusion tensor imaging (DTI) is a more recent MR imaging technique that assesses and quantifies water diffusion in biologic tissues at a microstructural level, taking advantage that water molecules diffuse more easily in the direction of the fibers than orthogonally, where they are hindered by oligodendroglial sheaths or axonal membranes.[3,4] This technique is therefore particularly suitable to study maturing axons,[5] even before myelination becomes evident on histologic examination.[6]

In the first DTI studies performed on neonates and infants, water diffusion changes were assessed through the placement of regions of interest (ROIs).[7-9] More sophisticated approaches used fiber bundle tractography to select regions where DTI values are expected to change with age.[10,11] These studies have shown that, for premature infants between ages 28 and 40 weeks, fractional anisotropy (FA), which expresses the fraction of the magnitude of the diffusion tensor attributable to anisotropic diffusion,[12] increases with age, whereas mean diffusivity (D_{av}), which corresponds to the directionally averaged magnitude of water diffusion, decreases with age in the white matter.[3,8,13] The increase in FA with age is explained by ensheathment of oligodendrocytes around axons, whereas a decrease in D_{av} relates to the "premyelination" stages (ie, isotropic proliferation of cells, intracellular compartments, and membranes).[7,14]

Approaches on the basis of ROIs have well-known limitations because strong a priori hypotheses about localization and extent of the effects of interest have to be made.[15] Voxel-based methods of neuroimaging data analysis, such as statistical parametric mapping (SPM), do not have such limitations and have been successfully applied to study age-related FA changes in adults, FA differences between preterm and full-term infants at term equivalent age, and brain structural asymmetries in infants.[16-20]

In this study, we combined SPM with probabilistic tractography to precisely identify the fiber tracts passing through the

Received February 13, 2009; accepted after revision April 17.

From the Departments of Pediatric Neurology (A.A., P.V.B.), Neuroradiology (Y.L., P.D., D.B., M.K., T.M.), and Laboratoire de Cartographie Fonctionnelle du Cerveau (X.D., P.V.B.), Université Libre de Bruxelles (ULB)-Hôpital Erasme, Brussels, Belgium; and Philips Healthcare Benelux (V.D.), Brussels, Belgium.

Previously presented at: International Society for Magnetic Resonance in Medicine Scientific Meeting and Exhibition, May 19–25, 2007, Berlin, Germany; Seventh European Pediatric Neurology Society Congress, September 26–29, 2007, Izmir, Turkey; Seventh International Congress on Early Brain Damage, April 23–26, 2008, Bled, Slovenia; and First Neuroimaging of Developmental Disorders, September 12–16, 2008, Dubrovnik, Croatia.

This research was supported by the 2007–2008 Belgacom research grant of the "Fonds Erasme pour la Recherche Médicale" (X. De Tiège) and the "Fonds Xénophilia, Fondation Roi Baudouin" (Y. Liu).

Please address correspondence to Alec Aeby, Department of Pediatric Neurology, ULB-Hôpital, Erasme, 808 route de Lennik, 1070 Brussels, Belgium; e-mail address: alec.aeby@ulb.ac.be

DOI 10.3174/ajnr.A1660

clusters of voxels experiencing significant FA changes with age in a group of healthy term and preterm infants.

Materials and Methods

Subjects

Among the population of infants prematurely born in our institution who did benefit from brain MR imaging investigation to detect lesions related to premature birth,[21] 26 infants (13 boys) born between 26.7 and 32 weeks of gestation were selected on the following criteria:

1. Normal weight and head circumference at birth for gestational age (>fifth and <95th percentiles).
2. Five-minute Apgar score of more than 6.
3. Lack of evidence of congenital infection or multiple congenital anomaly syndrome.
4. Normal results on structural brain MR imaging as assessed by a board-certificated neuroradiologist (P.D.).
5. Normal results on physical and neurologic examination at term-equivalent age and at 24 months corrected for gestational age as assessed by a board-certificated neuropediatrician (A.A.).
6. Normal psychomotor development at age 24 months corrected for gestational age as assessed by the Bayley III scale (mean ± 2 SDs).[22]
7. Echo-planar images (EPI) of good enough quality to perform DTI data processing (see further).

Eight healthy full-term babies (6 girls) born between 37.8 and 40.6 weeks of gestation completed the population. The initial population was thus composed of 34 preterm and full-term subjects. The Ethics Committee of our institution gave approval for the completion of this study (Reference: P2004/207). Informed written parental consent was obtained for each participant.

MR Imaging Data Acquisition

MR imaging investigations were performed on a 1.5T scanner equipped with an 8-channel sensitivity-encoding (SENSE) head coil. The following images were acquired for all subjects: 1) Sagittal 3D T1-weighted gradient-echo images: TR, 31 ms; TE, 4.6 ms; resolution, $0.8 \times 0.8 \times 1$ mm^3; number of sections, 100; FOV, 200 mm × 150 mm; section thickness, 1 mm; 2) Coronal T2-weighted turbo-spin-echo (TSE) images: TR, 11,741 ms; TE, 140 ms; TSE factor, 15; gap, 0.3 mm; number of sections, 40; FOV, 180 × 135 mm; section thickness, 3 mm; and 3) Spin-echo EPI: TR, 5888 ms; TE, 92 ms; FOV, 220 × 220 mm; 32 noncollinear diffusion-sensitizing gradient directions with diffusion sensitivity b of 600 s/mm;[23] a 2×2-mm^2 plane resolution; acceleration factor (SENSE), 2.2; section thickness, 2.3 mm.

Subjects were not sedated during image acquisition. To minimize movements that may distort signal intensity and therefore tensor estimation,[24] we performed MR imaging data acquisition early in the morning. When asleep, the subjects were positioned in a vacuum immobilization pillow to minimize body and head movements.[21] Earmuffs were placed to minimize noise discomfort.

DTI Data Processing for Parametric Studies

To minimize motion artifacts on tensor estimation, we defined our final study population using a 5-step strategy.

Step 1: Visual Inspection. EPI images (32 directions plus $b = 0$ s/mm^2) were visually inspected to search for the presence of motion artifacts (ie, signal intensity void, ghosting in at least one of the sections). Directions with motion artifacts were excluded from additional steps of data processing. No subject had motion artifacts in the $b = 0$ s/mm^2 or in more than 10 directions of the EPI images.

Step 2: Realignment. The diffusion tool of the SPM2 software package (Volkmar Glauche; SPM, Wellcome Department of Cognitive Neurology, Institute of Neurology, London, UK) was used to correct head movements.

The 32 directions (or 32-X_S directions, X_S expressing the number of directions removed for subject S in step 1) were realigned to the first diffusion-weighted volume. We corrected gradient orientations by applying the rotation matrix caused by the movement of the subject during MR imaging acquisition. The realigned volumes were resectioned, and the mean of the 32 (or 32-X_S) diffusion-weighted datasets was computed. Finally, the $b = 0$ s/mm^2 image was coregistered with this mean image and resectioned. Using this methodology, we created a full EPI dataset corrected for head movements, which were ready for DTI reconstruction and FA and D_{av} calculation.

Step 3: FA and D_{av} Calculation. We calculated FA and D_{av} using the diffusion tool of SPM2 on the basis of the maximal, intermediate, and minimal eigenvalues (λ_1, λ_2, λ_3), as proposed by Pierpaoli and Basser.[25]

Step 4: Image Normalization and Smoothing. Because automated and semi-automated MR imaging segmentation techniques were developed for volumetric T1 studies of the fully myelinated mature brain and are not directly transferable to the incompletely myelinated brain,[26] no segmentation procedure to separate gray and white matter was performed.[18,20] Images were spatially normalized in SPM2 with a reference template that consisted of the $b = 0$ s/mm^2 image of 1 healthy term subject who had no motion artifacts. The normalization used 12 degrees of freedom (translation, rotation, scale, and shear) and provided 45 FA sections composed of $2 \times 2 \times 2$-mm^3 voxels. Smoothing was then performed with an isotropic gaussian kernel of 5-mm full width at half maximum.[27]

We visually checked the anatomic accuracy of the spatial normalization using the "check registration" function of SPM2, which enabled us to compare the anatomic accuracy between subjects for several regions (posterior and anterior arms of the internal capsule, genu and splenium of the corpus callosum, and central part of the thalami).

Step 5: Quality Assessment of FA and D_{av} Maps. To assess the quality of the FA and D_{av} images obtained for our population after the first 4 processing steps, we performed a voxel-by-voxel 2-sample t test comparing FA and D_{av} images of each subject with the rest of the group. Results were considered significant at $P < .05$ corrected for multiple comparisons over the entire brain volume for clusters of more than 100 voxels. Subjects with significant results were excluded from the analysis.

Then, because withdrawal of 1 or more directions might modify FA and D_{av} values, we have estimated this modification for each case in which it was necessary to remove directions (see Step 1). Therefore, we have compared the FA and D_{av} values of the template subject in 5 polygonal ROIs (left and right posterior limbs of the internal capsule, genu of the corpus callosum, and left and right frontal lobe) calculated with 32 directions and with 32-X_S directions. Subjects were excluded from the parametric analysis if, in one of these 5 ROIs, the difference between FA and D_{av} values was larger than 5%.

Parametric Studies

We first considered the subject age when MR imaging was performed as the only covariate of interest, making the a priori hypothesis of a linear relationship between the variable and the regional FA and D_{av} changes. Because biologic changes may evolve nonlinearly during de-

velopment, we also used polynomial expansions to evidence nonlinear regression in parametric studies. We thus studied the second-order polynomial expansion of our parameter by defining the squared absolute value of the subject's age as a second covariate of interest.

The SPM(*F*), which is the image resulting from an *F*-statistic at every voxel, was obtained with a voxel height threshold of $P = .001$ (uncorrected). SPM(*F*) was analyzed in voxel-level statistical inference (ie, the probability that the observed voxel value could have occurred by chance in the volume analyzed). Only regions of more than 50 voxels attaining a corrected *P* value of less than .05 for this level of statistical inference were considered. Masks were used to exclude from the analysis corticospinal fluid and low signal-to-noise voxels ($FA < 0.1$ or $D_{av} > 2.10^{-3}$).[20] As we used the *F*-statistic, the positive or negative character of the significant linear or nonlinear relationship between FA and D_{av} values and age was determined by the slope of the regression plots between FA and D_{av} values and age obtained at each significant voxel.

Diffusion Tensor Tractography

We developed an original strategy to precisely identify the fiber tracts included in the brain regions to precisely show significant modification of FA with age.

Using adult neuroanatomy[28] and tractography atlases,[29] we selected fiber tracts suspected to be included in the significant voxels of the parametric studies. A multi-tensor probabilistic tractography[30] of these fiber tracts was performed on the template subject by use of the *Functional MR Imaging of the Brain Software Library* (FSL).[31] The obtained connectivity distributions were thresholded with a probability of 2%.

Coregistration of Parametric Maps and Tractography

We coregistered statistical parametric maps and all of the identified fiber tracts with the FA image of the template subject by using affine coregistration (FSL).

Results

DTI Data Processing for Parametric Studies

For 18 of the 34 subjects (12 premature and 6 term infants) motion artifacts were observed in at least one of the 32 directions acquired. Motion artifacts were encountered in 1 direction for 1 subject, 2 directions for 3 subjects, 3 directions for 4 subjects, 4 directions for 4 subjects, 5 directions for 4 subjects, 7 directions for 1 subject, and 9 directions for 1 subject. These 18 subjects were homogeneously distributed according to the age of gestation at the time of MR imaging.

Among the 34 subjects, the 2-sample *t* tests comparing each patient with the rest of the group revealed significant FA clusters in 4 subjects. These subjects were excluded for further analysis.

Two additional subjects were excluded because the difference in the FA value of the template subject calculated with 32 directions and 32-X_S directions was larger than 5% in at least one of the 5 ROIs.

The population available for parametric studies was thus composed of 28 subjects (22 premature and 6 term infants) scanned between 34 and 41 weeks. Gestational age when MR imaging was performed was 39.4 ± 1.2 weeks for the full-term population and 36.3 ± 0.9 weeks for the preterm population.

Parametric Studies

Parametric studies showed a strong statistical correlation between the subjects' age and FA in various subcortical structures. Significant clusters were found in the subcortical projection pathways of the frontal (motor and premotor areas) and parietal cortices, the centrum semiovale, the anterior and posterior arms of the internal capsules, the optic radiations, the splenium, and the genu of the corpus callosum and the thalami (Fig 1). The positive slope of the regression plot obtained in the subcortical projection pathways of the right frontal motor cortex, where the *F*-value was the highest ($F = 59.63$), indicated an FA increase with increasing age (Fig 2). The same type of correlation was observed in all of the other statistically significant regions. The second-order polynomial expansion (highest *F*-value = 29.30) did not indicate nonlinear FA increase with age. No statistically significant results were found for D_{av} maps.

Diffusion Tensor Tractography

On the basis of neuroanatomic and tractography atlases, we identified the corticospinal tract (CST); the thalamic radiations, which are divided into the superior thalamic radiations (STR), anterior thalamic radiations (ATR), and posterior thalamic radiations (PTR); and the callosal radiations (CR) as the fiber tracts possibly included in the significant clusters of the parametric analysis. To confirm this hypothesis, we processed the template used for normalization with a seed mask positioned in the mesencephalon and a waypoint mask in the precentral gyrus to track the CST.[32] The anterior and posterior parts of the STR were tracked between the seed mask positioned in the thalamus on the axial image and the waypoint mask covering the precentral and postcentral gyri above the corpus callosum.[33] The same thalamic seed mask as used for the STR was used to track the fibers of the ATR and PTR, with the waypoint masks placed in the frontal and occipital lobes, respectively.[33]

Coregistration of Parametric Maps and Tractography

The coregisteration of the parametric maps and probabilistic tractography showed that the CST, the STR, the PTR, the ATR, and the CR (Fig 3) were included in the significant clusters, confirming that significant FA increase does occur in these tracts between 34 and 41 weeks of gestation. Regression plots of FA with gestational age in all of the above-mentioned tracts and the thalamus on the right hemisphere are given in Fig 2. Similar regression plots were obtained for the left hemisphere.

Discussion

We used a voxel-based approach to identify FA changes in a population of healthy preterm and term infants and found that FA increases between 34 and 41 weeks in the thalami, the subcortical projection pathways of the frontal (motor and premotor) and parietal cortices, the centrum semiovale, the anterior and posterior arms of internal capsules, the corpus callosum, and the optic radiations. We reconstructed the suspected fiber tracts included in the significant clusters using probabilistic tractography and superimposed them on the parametric maps, which enabled us to conclude that the thalamic radiations, the CR, and the CST experience microstructural changes between 34 and 41 weeks of gestation.

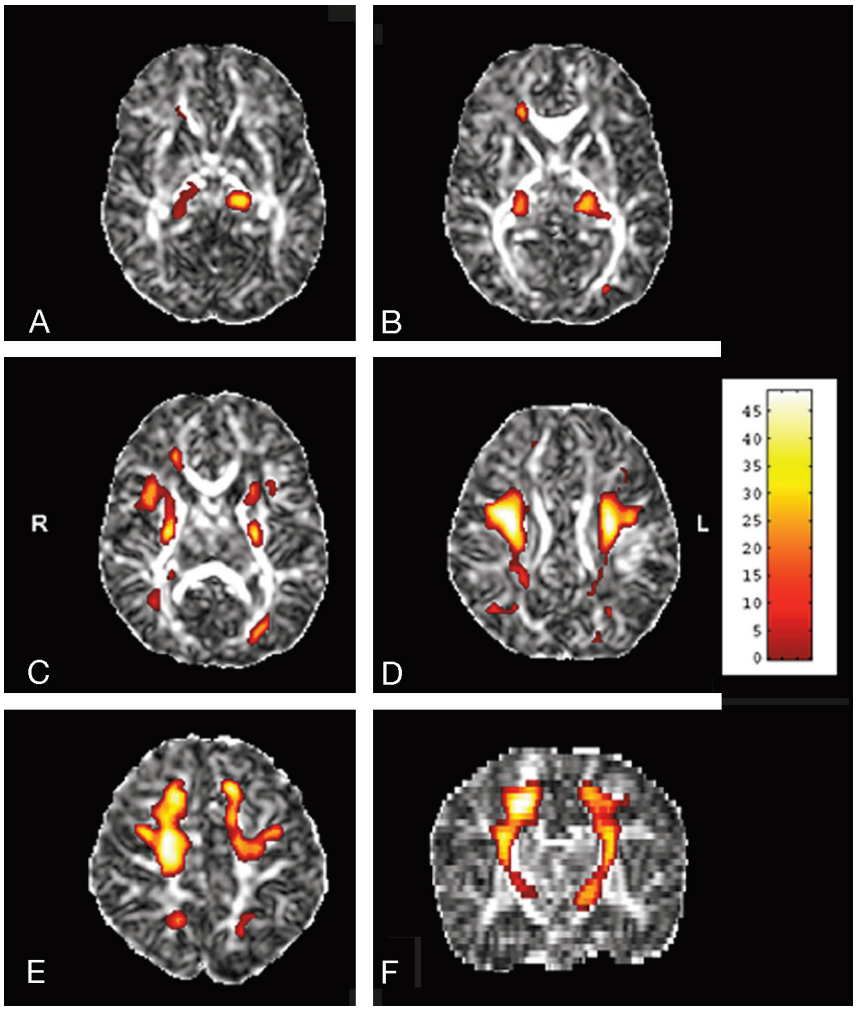

Fig 1. Areas with significant FA increase with age are located in the thalami (*A, B*), the anterior and posterior arms of the internal capsules, and the optic radiations (*C*), the centrum semiovale (*D*), and the subcortical projection pathways of the frontal and parietal cortices (*E*) in the axial (*A–E*) and coronal (*F*) planes. The anatomic underlay is the FA image of the template. The color maps represent the *F*-scores. Only regions of more than 50 voxels attaining a corrected *P* value of less than .05 for the voxel-level of statistical inference were considered significant.

Proof of FA increase in the thalami with increasing age from 34 weeks is original and in agreement with studies showing that FA increases with age in the somatosensory tracts and in the optic radiations, which are part of the STR and PTR, respectively.[8,13,34-36] Structural modification of these fibers is also supported by neurophysiologic studies showing reduced latencies of somatosensory and visual-evoked responses with increasing age in neonates.[37,38] Thalamic radiations start to develop in the brain between 20 and 23 weeks of gestation when they reach the superficial part of the subplate zone.[39] Between 24 and 32 weeks of gestation, axons grow from the subplate zone to the cortical plate and develop synapses in the deep cortical plate.[39,40] This developmental stage is characterized by the first appearance of 2 parallel and concurrent functional circuits in the neocortex: the thalamocortical loop and the endogenous and spontaneously active circuitry of the subplate zone, which will tend to disappear at approximately 38 weeks of gestation.[41] The spatial resolution of our system did not allow us to identify which thalamic nuclei did experience significant changes. We could speculate that, because the thalamus via the thalamic radiations is known to be an integrative center for regulation of sensorimotor functions and states of consciousness,[42] its maturation could contribute to the improvement of the quality of movements, level of alertness, and visual function that neonates experience between 34 and 41 weeks of gestation.[43]

The FA increase in the CST and CR has already been described by several authors.[7,8] Anatomopathologic studies have shown that between 34 and 41 weeks of gestation, the CST will experience significant maturational changes.[44] This is in agreement with the observation during that period of a switch of the control of movements from the subcorticospinal motor system to the corticospinal system, leading to more organized and fluid motor behavior.[43]

The posterior limb of the internal capsule starts to myelinate at 36 weeks, and other regions where we found FA increase with gestational age (ie, the thalami, the supracapsular portion of the CST and STR, the ATR and the PTR in the CR) are not yet myelinated at 41 weeks.[44] Therefore, besides myelination,[14] the FA increase in these tracts and regions probably also relates to unmyelinated oligodendrocyte ensheathment around the axons. It is interesting to note that Drobyshevsky et al[45] recently reported that, in the brain of rabbit, developmental changes in anisotropy coincide with proliferation of immature oligodendrocytes before myelination. Myelination is known to spread from the central to the peripheral regions

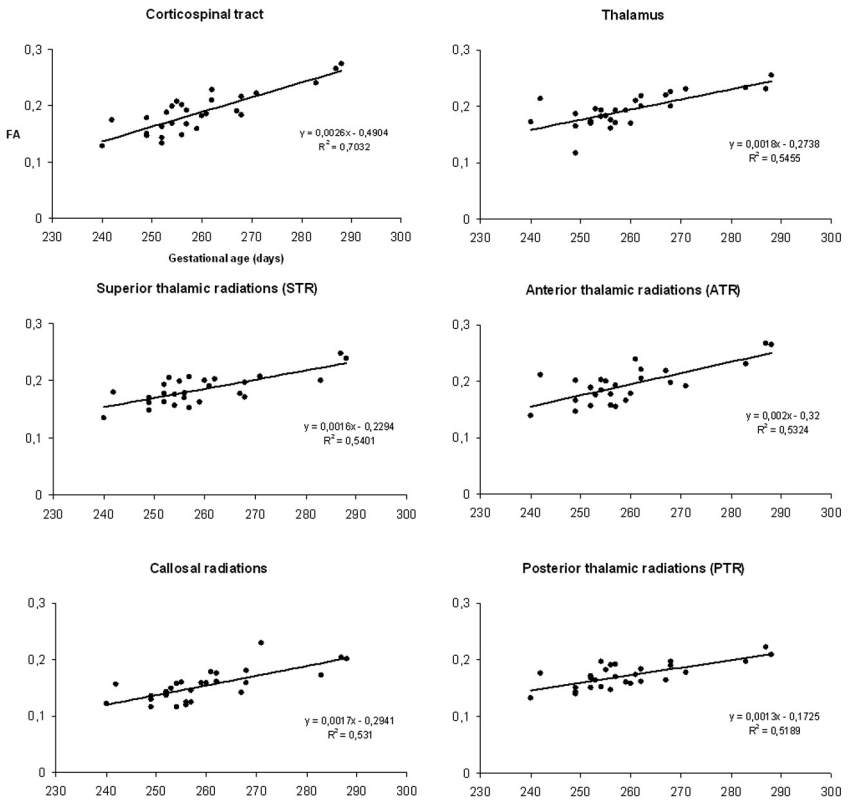

Fig 2. Regression plots derived from gestational age in relationship to FA values at the most statistically significant voxels located in the CST ($F = 59.63$), the thalamus ($F = 31.23$), the STR ($F = 30.54$), the ATR ($F = 29.61$), the CR ($F = 29.44$), and the PTR ($F = 25.27$) on the right side of the brain. The positive slopes of the regression lines indicate that FA increases with age.

and from the central sulcus outward to the poles.[14] As most of the significant voxels of our analysis were centrally located in the brain (Fig 3), FA increase between 34 and 41 weeks of gestation seems to follow the same spatiotemporal progression as myelination, but somewhat earlier.

Many significant voxels were not included in the tracts reconstructed with use of probabilistic fiber tractography. These voxels could still correspond, in our opinion, to subcortical projection pathways of the CST, thalamic radiations, and CR not evidenced by tractography. Indeed, the low FA value in neonate brains might have decreased the actual size of the reconstructed bundles.[8] Another possibility is that the 2D ROI method we used limited reconstruction to the part of the tract that crosses the selected ROIs. For example, for the CST, 2D ROIs tend to find only projections in the superior-inferior direction (medial portion of the motor tract), missing the left-right direction (lateral portions of the tract). It has been suggested that 3D ROIs with use of cortical masks that include the whole motor cortex for the CST could resolve this limitation in adults.[11] Nevertheless, because cortical masking implies a good contrast between gray and white matter to define the mask, this technique seems difficult to apply in a neonate population.

We did not find significant changes in D_{av} with age in our group of subjects. This is in agreement with other studies showing that FA is more sensitive to detect differences between tracts in the premature brain.[8,46,47] It was proposed that the expansive nonlinearity at low anisotropy values provided by the FA index might better distinguish small differences in anisotropy in the neonatal brain compared with the more linear D_{av} index.[12] Because the D_{av} decrease relates essentially to isotropic proliferation of cells, intracellular compartments, and membranes,[14] we can speculate that brain maturation between 34 and 41 weeks of gestational age is mainly anisotropic.

Some methodologic issues deserve special comments. First, the use of SPM in DTI studies has been questioned by authors considering that changes observed could be the result of local misalignment and not changes in white matter microstructure.[48] To take into account this criticism, results of the spatial normalization were visually verified for several brain structures. Tract-based spatial statistics, which are also an automated, observer-independent approach for the assessment of FA on a voxel-wise basis across groups of subjects,[48] could resolve some of these problems via carefully tuned nonlinear registration of FA images followed by projection onto an alignment-invariant tract representation (the "mean FA skeleton"). Nevertheless, this technique restricts the analysis to major white matter tracts, excluding central gray matter such as the thalami, and is not easily applicable to neonates because of low FA values of the immature brain.

A second issue concerns movement artifacts during acquisition, which is a recurrent problem when performing DTI studies in nonsedated neonates. In our study, DT images with motion artifacts were rejected. Because rejecting directions might modify FA values, we rejected patients with more than 5% FA value modification induced by direction removal, so we are confident that our results were biased neither by motion artifacts nor by the error resulting from rejecting direc-

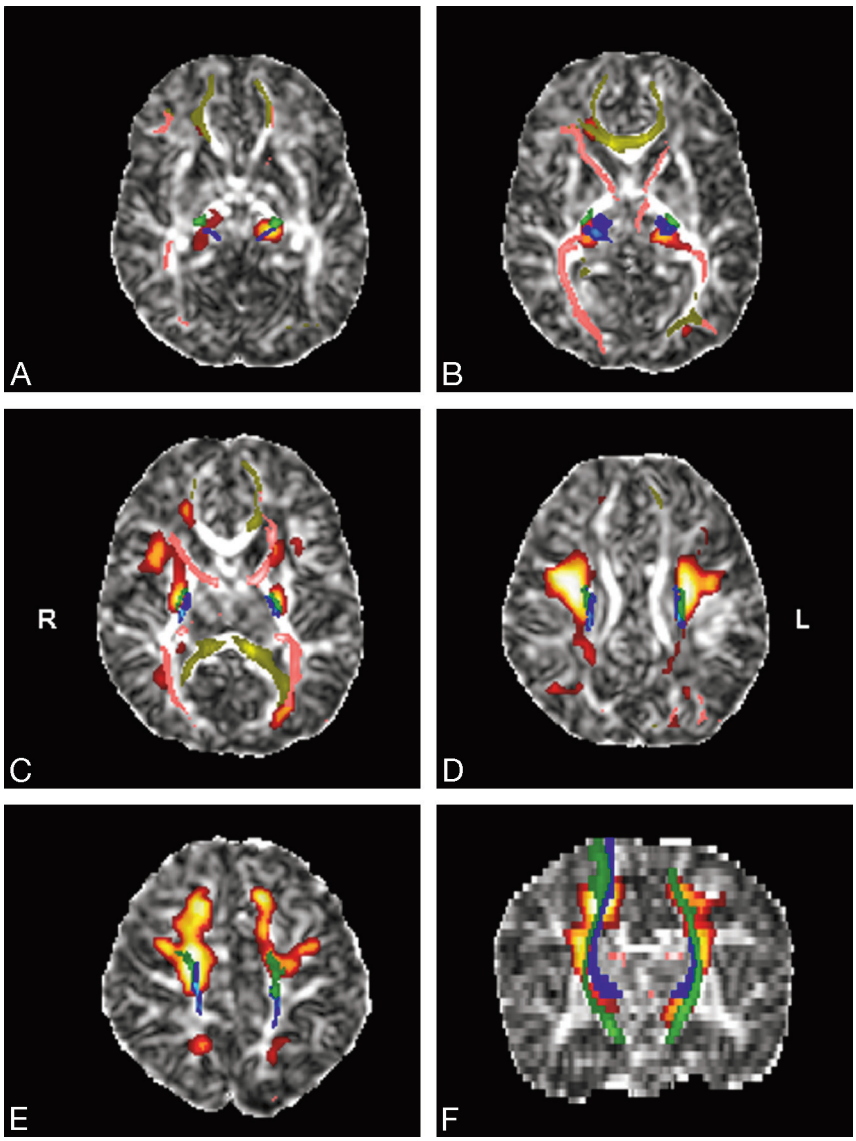

Fig 3. Superimposition of statistical parametric maps (*red-orange*), probabilistic tractography images (*blue, green, pink, yellow*), and FA images of the template in the axial (*A–E*) and coronal (*F*) planes. The CST (*green*), the STR (*blue*), the ATR, the PTR (*pink*), and the CR (*yellow*) are included in the significant voxels of the parametric analysis.

tions. A last issue concerns the population studied, which is composed of healthy term babies and preterm babies considered as healthy. The normality of our preterm population was based on robust structural and clinical criteria. Nevertheless, we cannot exclude that some of the premature infants might have subtle cognitive deficits associated with abnormal FA values in several regions. Studies have shown altered white matter diffusion anisotropy in preterm compared with normal-term infants, but it should be emphasized that results differ from 1 study to another.[7,19,49,50] Moreover, if subtle white matter lesions had occurred in some of the children born prematurely, it is unlikely that they would be distributed homogeneously and symmetrically in all of the regions so that linear FA increases with age would not be found.

Conclusions

In this combined study of voxel-based analysis and probabilistic tractography with use of DTI, we could evidence that, besides regions previously identified by ROI- and tractography-based analyses, significant maturational changes do occur in the thalami and in the thalamic radiations in neonates between 34 and 41 weeks of gestation. We also showed that FA increases in brain regions where myelin is not present yet, suggesting that a FA increase with age also relates to unmyelinated oligodendrocyte ensheathment around axons. The clinical impact of an impairment of this process in motor and cognitive handicaps needs to be studied.

Acknowledgments

We thank the parents of the subjects for accepting that their children participate in the study; M. Creuzil, psychologist, for performing Bayley III scale to the subjects; A. Pardou, head of the Neonatal Intensive Care Unit of Erasme Hospital, for helping us to recruit subjects; C.A. Clarck, Institute of Child Health, London, UK, for methodological support; and M.

Gassner, Universitè Libre de Bruxelles, for reviewing the manuscript.

References

1. Sidman RL, Rakic, P. **Development of the human nervous system.** In: Haymaker W, Adams, R.D, ed. *Histology and Histopathology of the Nervous System.* Springfield: Charles C. Thomas, 1982:3–145
2. Paus T, Collins DL, Evans AC, et al. **Maturation of white matter in the human brain: a review of magnetic resonance studies.** *Brain Res Bull* 2001;54:255–66
3. Huppi PS, Dubois J. **Diffusion tensor imaging of brain development.** *Semin Fetal Neonatal Med* 2006;11:489–97
4. Jellison BJ, Field AS, Medow J, et al. **Diffusion tensor imaging of cerebral white matter: a pictorial review of physics, fiber tract anatomy, and tumor imaging patterns.** *AJNR Am J Neuroradiol* 2004;25:356–69
5. Basser PJ, Pierpaoli C. **Microstructural and physiological features of tissues elucidated by quantitative-diffusion-tensor MRI.** *J Magn Reson B* 1996;111:209–19
6. Wimberger DM, Roberts TP, Barkovich AJ, et al. **Identification of "premyelination" by diffusion-weighted MRI.** *J Comput Assist Tomogr* 1995;19:28–33
7. Huppi PS, Maier SE, Peled S, et al. **Microstructural development of human newborn cerebral white matter assessed in vivo by diffusion tensor magnetic resonance imaging.** *Pediatr Res* 1998;44:584–90
8. Partridge SC, Mukherjee P, Henry RG, et al. **Diffusion tensor imaging: serial quantitation of white matter tract maturity in premature newborns.** *Neuroimage* 2004;22:1302–14
9. Neil J, Miller J, Mukherjee P, et al. **Diffusion tensor imaging of normal and injured developing human brain—a technical review.** *NMR Biomed* 2002;15:543–52
10. Conturo TE, Lori NF, Cull TS, et al. **Tracking neuronal fiber pathways in the living human brain.** *Proc Natl Acad Sci U S A* 1999;96:10422–27
11. Behrens TE, Johansen-Berg H, Woolrich MW, et al. **Non-invasive mapping of connections between human thalamus and cortex using diffusion imaging.** *Nat Neurosci* 2003;6:750–57
12. Ulug AM, van Zijl PC. **Orientation-independent diffusion imaging without tensor diagonalization: anisotropy definitions based on physical attributes of the diffusion ellipsoid.** *J Magn Reson Imaging* 1999;9:804–13
13. Berman JI, Mukherjee P, Partridge SC, et al. **Quantitative diffusion tensor MRI fiber tractography of sensorimotor white matter development in premature infants.** *Neuroimage* 2005;27:862–71
14. Dubois J, Dehaene-Lambertz G, Perrin M, et al. **Asynchrony of the early maturation of white matter bundles in healthy infants: quantitative landmarks revealed noninvasively by diffusion tensor imaging.** *Hum Brain Mapp* 2008;29:14–27
15. Giuliani NR, Calhoun VD, Pearlson GD, et al. **Voxel-based morphometry versus region of interest: a comparison of two methods for analyzing gray matter differences in schizophrenia.** *Schizophr Res* 2005;74:135–47
16. Ashtari M, Cervellione KL, Hasan KM, et al. **White matter development during late adolescence in healthy males: a cross-sectional diffusion tensor imaging study.** *Neuroimage* 2007;35:501–10
17. Camara E, Bodammer N, Rodriguez-Fornells A, et al. **Age-related water diffusion changes in human brain: a voxel-based approach.** *Neuroimage* 2007;34:1588–99
18. Snook L, Plewes C, Beaulieu C. **Voxel based versus region of interest analysis in diffusion tensor imaging of neurodevelopment.** *Neuroimage* 2007;34:243–52
19. Gimenez M, Miranda MJ, Born AP, et al. **Accelerated cerebral white matter development in preterm infants: a voxel-based morphometry study with diffusion tensor MR imaging.** *Neuroimage* 2008;41:728–34
20. Dubois J, Hertz-Pannier L, Cachia A, et al. **Structural asymmetries in the infant language and sensori-motor networks.** *Cereb Cortex* 2009;19:414–23
21. Woodward LJ, Anderson PJ, Austin NC, et al. **Neonatal MRI to predict neurodevelopmental outcomes in preterm infants.** *N Engl J Med* 2006;355:685–94
22. Bayley N. *Manual for the Bayley Scales of Infant Development, 3d ed.* San Antonio: Psychological Corporation; 2005
23. Jones DK, Horsfield MA, Simmons A. **Optimal strategies for measuring diffusion in anisotropic systems by magnetic resonance imaging.** *Magn Reson Med* 1999;42:515–25
24. Dubois J, Poupon C, Lethimonnier F, et al. **Optimized diffusion gradient orientation schemes for corrupted clinical DTI data sets.** *Magma* 2006;19:134–43
25. Pierpaoli C, Basser PJ. **Toward a quantitative assessment of diffusion anisotropy.** *Magn Reson Med* 1996;36:893–906
26. Nishida M, Makris N, Kennedy DN, et al. **Detailed semiautomated MRI based morphometry of the neonatal brain: preliminary results.** *Neuroimage* 2006;32:1041–49
27. Jones DK, Symms MR, Cercignani M, et al. **The effect of filter size on VBM analyses of DT-MRI data.** *Neuroimage* 2005;26:546–54
28. Greenstein BG. *Color Atlas of Neuroscience: Neuroanatomy and Neurophysiology.* Stuttgart: Thieme; 2000
29. Wakana S, Jiang H, Nagae-Poetscher LM, et al. **Fiber tract-based atlas of human white matter anatomy.** *Radiology* 2004;230:77–87
30. Behrens TE, Berg HJ, Jbabdi S, et al. **Probabilistic diffusion tractography with multiple fibre orientations: What can we gain?** *Neuroimage* 2007;34:144–55
31. Smith SM, Jenkinson M, Woolrich MW, et al. **Advances in functional and structural MR image analysis and implementation as FSL.** *Neuroimage* 2004;23 Suppl 1:S208–219
32. Thomas B, Eyssen M, Peeters R, et al. **Quantitative diffusion tensor imaging in cerebral palsy due to periventricular white matter injury.** *Brain* 2005;128:2562–77
33. Mori S, van Zijl PC. **Fiber tracking: principles and strategies—a technical review.** *NMR Biomed* 2002;15:468–80
34. Dubois J, Hertz-Pannier L, Dehaene-Lambertz G, et al. **Assessment of the early organization and maturation of infants' cerebral white matter fiber bundles: a feasibility study using quantitative diffusion tensor imaging and tractography.** *Neuroimage* 2006;30:1121–32
35. Gilmore JH, Lin W, Corouge I, et al. **Early postnatal development of corpus callosum and corticospinal white matter assessed with quantitative tractography.** *AJNR Am J Neuroradiol* 2007;28:1789–95
36. Hermoye L, Saint-Martin C, Cosnard G, et al. **Pediatric diffusion tensor imaging: normal database and observation of the white matter maturation in early childhood.** *Neuroimage* 2006;29:493–504
37. Crognale MA, Kelly JP, Chang S, et al. **Development of pattern visual evoked potentials: longitudinal measurements in human infants.** *Optom Vis Sci* 1997;74:808–15
38. McCulloch DL, Orbach H, Skarf B. **Maturation of the pattern-reversal VEP in human infants: a theoretical framework.** *Vision Res* 1999;39:3673–80
39. Kostovic I, Rakic P. **Developmental history of the transient subplate zone in the visual and somatosensory cortex of the macaque monkey and human brain.** *J Comp Neurol* 1990;297:441–70
40. Kostovic I, Jovanov-Milosevic N. **The development of cerebral connections during the first 20–45 weeks' gestation.** *Semin Fetal Neonatal Med* 2006;11:415–22
41. Kostovic I, Judas M. **Prolonged coexistence of transient and permanent circuitry elements in the developing cerebral cortex of fetuses and preterm infants.** *Dev Med Child Neurol* 2006;48:388–93
42. Parent A. *Carpenter's Human Neuroanatomy, 9th ed.* Baltimore: Williams and Wilkins; 1996
43. Saint-Anne Dargassies S. *Neurological Development in the Full-Term and Premature Neonate.* New York: Excerpta Medica; 1977
44. Brody BA, Kinney HC, Kloman AS, et al. **Sequence of central nervous system myelination in human infancy. I. An autopsy study of myelination.** *J Neuropathol Exp Neurol* 1987;46:283–301
45. Drobyshevsky A, Song SK, Gamkrelidze G, et al. **Developmental changes in diffusion anisotropy coincide with immature oligodendrocyte progression and maturation of compound action potential.** *J Neurosci* 2005;25:5988–97
46. Vangberg TR, Skranes J, Dale AM, et al. **Changes in white matter diffusion anisotropy in adolescents born prematurely.** *Neuroimage* 2006;32:1538–48
47. Skranes J, Vangberg TR, Kulseng S, et al. **Clinical findings and white matter abnormalities seen on diffusion tensor imaging in adolescents with very low birth weight.** *Brain* 2007;130:654–66
48. Smith SM, Jenkinson M, Johansen-Berg H, et al. **Tract-based spatial statistics: voxelwise analysis of multi-subject diffusion data**. *Neuroimage* 2006;31:1487–505
49. Anjari M, Srinivasan L, Allsop JM, et al. **Diffusion tensor imaging with tract-based spatial statistics reveals local white matter abnormalities in preterm infants.** *Neuroimage* 2007;35:1021–27
50. Rose SE, Hatzigeorgiou X, Strudwick MW, et al. **Altered white matter diffusion anisotropy in normal and preterm infants at term-equivalent age.** *Magn Reson Med* 2008;60:761–67